

## A HYBRID METHOD OF SCATTERING FROM A DIELECTRIC TARGET ABOVE A ROUGH SURFACE: TE CASE

Lin Li<sup>\*</sup>, Tian Lin Dong, and Qing Xia Li

Department of Electronics and Information, Huazhong University of Science and Technology, No. 1037, Luoyu Ave., Wuhan 430074, P. R. China

**Abstract**—A hybrid method, combining analytic Kirchhoff approximation (KA) and numerical method of moments (MoMs), is developed to solve the two-dimensional (2D) scattering problem of a dielectric target with arbitrary cross section above a moderate perfect electric conductor (PEC) rough surface under TE-polarized tapered wave incidence. The induced current on the rough surface is analytically expressed using the KA method, which depends on the tapered incident wave and the field illuminating by current distribution on the target, leaving only unknown induced current on the target. So the electric field integral equations of the induced currents on the target only can be derived; it allows a substantial reduction of computation time and memory requirement. Furthermore, for different secondary scattering of the underlying rough surface, different truncations of the rough surface are taken to speed up computation of the scattering contribution from the rough surface to the target. Making use of Monte Carlo realization, bistatic scattering from a cylindrical target above a PEC rough surface is well simulated to test validity and efficiency of the proposed method. Numerical results from the hybrid method have good agreements with those from the conventional method of moments. However, the computational time and the memory requirements have been greatly reduced.

---

*Received 8 April 2013, Accepted 27 May 2013, Scheduled 30 May 2013*

\* Corresponding author: Lin Li (lilin2008@smail.hust.edu.cn).

## 1. INTRODUCTION

Electromagnetic scattering from the composite model of a target above a rough surface has attracted great interest in recent years [1–20]. The study of such an electromagnetic scattering problem is a complex and difficult subject due to the difficulty in calculating the coupling scattering between the target and the rough surface. Up to now, the methods for this subject can be cataloged as three kinds: the analytic methods [1, 2], the numerical methods [3–14] and hybrid methods which combine the analytic method and the numerical method [15–20]. The analytic method is of high efficiency but restricted to some regular cases. For the numerical methods although there are many accelerate algorithms, such as general forward backward method and spectrum acceleration algorithm (GFBM/SAA) [4, 5], finite element method and domain decomposition method (FEM-DDM) [6], multilevel fast multipole algorithm (MLFMA) [7, 8], extended propagation-inside-layer expansion (PILE) method combined with forward-backward spectral acceleration (FB-SA) [9, 10], cross coupling iterative approach combining the conjugate gradient method (CG) and the forward and backward method [11–13], they all generate a large scale of unknowns from the target and the rough surface discretization for a desired accuracy. To overcome the disadvantage of both the analytic and numerical methods, there comes the hybrid method. Recently, many hybrid methods have been developed, such as the hybrid SPM/MoM technique [15], hybrid MM-PO combining UV technique [16], iterative hybrid method combining analytic KA and numerical MoM [17], current based hybrid KA/MoM method [18], iterative hybrid method combining KA and MLFMA [19], hybrid method combining KA, third-order equivalent edge currents for physical theory of diffraction (PTDEEC), method of equivalent edge currents (MEC), and the reciprocity theorem [20]. But they are all about PEC target above a rough surface, so far little work has been done about hybrid method of scattering from dielectric target above a rough surface.

In this paper, the current based hybrid method for scattering from a dielectric target above a PEC rough surface under TE-polarized tapered wave incidence is proposed, in which there are only unknown induced currents on the target while the induced currents on the rough surface can be directly calculated by the tapered incident wave and the induced currents on the target. Numerical results are given to illustrate the validity and efficiency of the proposed method.

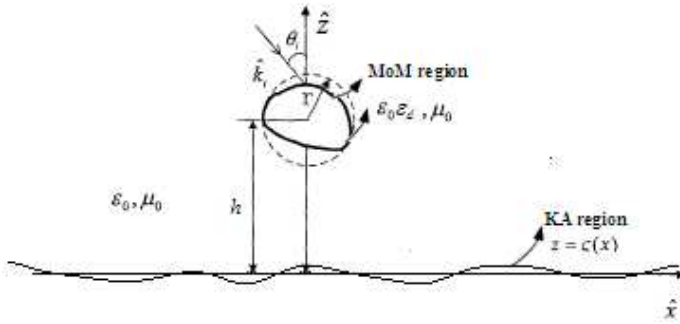


**Figure 1.** Model of a dielectric target above a rough surface.

## 2. CONFIGURATION AND FORMULATION

Figure 1 illustrates the basic geometry considered in this paper: a dielectric target with complex permittivity  $\epsilon_0\epsilon_d$  is located at altitude  $h$  above a moderate PEC rough surface which satisfies the conditions for validity of the Kirchhoff approximation [21] ( $k_0l > 6$ ,  $l^2 > 2.76\delta\lambda$ ), where  $k_0$  is the wavenumber of free space,  $l$  the correlation length,  $\lambda$  the incident wavelength, and  $\delta$  the RMS height.  $r$  is the radius of the target envelop indicated by the dashed line.

### 2.1. EFIEs of the Induced Currents on the Target

Suppose a TE tapered wave is incident on the target and the underlying surface along  $\widehat{k}_i = \widehat{x} \sin \theta_i - \widehat{z} \cos \theta_i$ . The tapered wave is expressed as

$$E_i(\vec{r}) = \exp(-jk_0(x \sin \theta_i - z \cos \theta_i) \cdot (1 + w(\vec{r}))) \cdot \exp\left(-\frac{(x + z \tan \theta_i)^2}{g^2}\right) \quad (1)$$

$$w(\vec{r}) = \frac{2\frac{(x+z \tan \theta_i)^2}{g^2} - 1}{(k_0g \cos \theta_i)^2} \quad (2)$$

with  $g$  the tapering parameter. According to the previous papers [11, 22], tapering parameter  $g$  and surface length  $L$  should satisfy all requirements of the wave equation, correlation length, energy truncation and the largest scattering angle  $\theta_m$  in bistatic normalized radar cross section (Bi-NRCS) calculation, which can be expressed as

$$g > \frac{6}{(\cos \theta_i)^{1.5}} \quad (3)$$

$$L \geq 15lc \quad (4)$$

$$L \geq 4g \quad (5)$$

$$L \geq 2 \left( \frac{r}{\cos \theta_m} + h \tan \theta_m \right) \quad (6)$$

Moreover, in order to ensure not only enough illuminated intensity over the target but also enough scattering intensity from the underlying surface to the target,  $g$  would be taken as [11, 12]

$$g \geq 4 \left( \frac{r}{\cos \theta_i} + h \tan \theta_i \right) \quad (7)$$

Then subdivided the target surface into  $N$  segments and the rough surface  $P$  segments, where the pulse width on the target is  $\lambda/15$  and the horizontal pulse width on the rough surface is  $\lambda/10$  respectively. In this composite model due to the incident tapered electric field and the coupling scattering between the target and the rough surface, the induced current  $J_s$  on the rough surface, electric current  $J_o$  and magnetic current  $K_o$  on the target surface can be driven and expressed as linear superposition of pulse basis functions

$$\mathbf{J}_s = \hat{y} \sum_{p=1}^P J_{sp} f_p \quad (8)$$

$$\mathbf{J}_o = \hat{y} \sum_{n=1}^N J_{on} f_n \quad (9)$$

$$\mathbf{K}_o = \sum_{n=1}^N \hat{t}_n K_{on} f_n \quad (10)$$

where  $\hat{t}_n$  is the clockwise unit vector at the middle of the  $n$ th segment tangent to target surface. The scattered field of the target is produced by the induced currents on the target [23], written as

$$\mathbf{E}_{\text{so}}(\bar{\mathbf{r}}) = \hat{y} E_{so}(\bar{\mathbf{r}}) = \hat{y} \left\{ ik_0 \eta_0 A_o(\bar{\mathbf{r}}) - \left( \frac{\partial F_x(\bar{\mathbf{r}})}{\partial z} - \frac{\partial F_z(\bar{\mathbf{r}})}{\partial x} \right) \right\}, \quad (11)$$

where  $\eta_0$  is the intrinsic impedance of free space, and

$$A_o(\bar{\mathbf{r}}) = \int_c J_o(\bar{\mathbf{r}}') \frac{i}{4} H_0^{(1)}(k_0 R) d\bar{\mathbf{r}}', \quad (12)$$

$$F_o(\bar{\mathbf{r}}) = \int_c K_o(\bar{\mathbf{r}}') \frac{i}{4} H_0^{(1)}(k_0 R) d\bar{\mathbf{r}}', \quad (13)$$

where  $R = |\bar{\mathbf{r}} - \bar{\mathbf{r}}'|$  is the distance between the source point and field point, and the integration  $d\bar{\mathbf{r}}'$  is along the contour of the target

(denoted by  $c$ ). Then in the composite target/surface model the incident field to the underlying surface takes the incident tapered wave and the scattering field from the target into account

$$E^{in}(\bar{r}) = E_i(\bar{r}) + E_{so}(\bar{r}), \quad \bar{r} \in S \quad (14)$$

Using KA [21, 24], the field on the underlying surface can be expressed as

$$\frac{\partial E_S(\bar{r})}{\partial n} = 2 \frac{\partial E^{in}(\bar{r})}{\partial n} = -ik_0\eta_0 J_s, \quad \bar{r} \in S \quad (15)$$

In contrast to the numerical method, the induced current  $J_s$  on the rough surface are not based on the solution of a system of linear equations, they are determined by the tapered wave and the scattering field contributed by the  $J_o$  and  $K_o$  on the target as

$$J_s = \sum_{p=1}^P \frac{i \left( 2 \frac{\partial E_i(r_p)}{\partial n} + 2 \frac{\partial E_{so}(r_p)}{\partial n} \right)}{k_0\eta_0} f_p, \quad (16)$$

From Equations (11)–(13) and (16), the induced current on the rough surface can be expressed as

$$[J_s] = [J_i] + [ZJ][J_o] + [ZK][K_o], \quad (17)$$

where

$$J_i = \sum_{p=1}^P \frac{2i \frac{\partial E_i(r_p)}{\partial n}}{k_0\eta_0} f_p, \quad (18)$$

$$ZJ_{pn} = -\frac{i}{2} \frac{\partial H_0^{(1)}(k_0 |\bar{r}_p - \bar{r}_n|) d\bar{r}'_n}{\partial n} \Big|_{\bar{r}=\bar{r}_p}, \quad (19)$$

$$ZK_{pn} = -\frac{\partial \left( \hat{t}_n \cdot \hat{x} \frac{\partial H_0^{(1)}(k_0 |\bar{r}_p - \bar{r}_n|) d\bar{r}'_n}{\partial z} \Big|_{z=z_p} - \hat{t}_n \cdot \hat{z} \frac{\partial H_0^{(1)}(k_0 |\bar{r}_p - \bar{r}_n|) d\bar{r}'_n}{\partial x} \Big|_{x=x_p} \right)}{2k_0\eta_0 \partial n} \Big|_{\bar{r}=\bar{r}_p} \quad (20)$$

From Equation (17), the induced current on the rough surface can be directly calculated by matrix equation of electric current and magnetic current on the target. Then the electric field integral equations (EFIEs) on the target can be derived as

$$E_i(\bar{r}) + ik_0\eta_0 A_s(\bar{r}) + ik_0\eta_0 A_o(\bar{r}) - \left( \frac{\partial F_x(\bar{r})}{\partial z} - \frac{\partial F_z(\bar{r})}{\partial x} \right) = K_o(\bar{r})(\bar{r} \in c^+), \quad (21)$$

$$ik_d\eta_d A_o^{(d)}(\bar{r}) - \left( \frac{\partial F_x^{(d)}(\bar{r})}{\partial z} - \frac{\partial F_z^{(d)}(\bar{r})}{\partial x} \right) = -K_o(\bar{r})(\bar{r} \in c^-), \quad (22)$$

$$A_s(\bar{r}) = \int_S J_s(\bar{r}') \frac{i}{4} H_0^{(1)}(k_0 R) d\bar{r}', \quad (23)$$

$$A_o^{(d)}(\bar{r}) = \int_c J_o(\bar{r}') \frac{i}{4} H_0^{(1)}(k_d R) d\bar{r}', \quad (24)$$

$$\bar{F}^{(d)}(\bar{r}) = \int_c \hat{t} K_o(\bar{r}') \frac{i}{4} H_0^{(1)}(k_d R) d\bar{r}', \quad (25)$$

where  $k_d = k_0 \sqrt{\varepsilon_d}$  and  $\eta_d = \eta_0 / \sqrt{\varepsilon_d}$  are, respectively, the wavenumber and impedance in the dielectric target, and  $\varepsilon_d$  is the target relative permittivity. The second item in the left side of the equation which is the underlying rough surface scattering account to the target can be expressed as

$$ik_0 \eta_0 A_s(\bar{r}) = [Z][J_{sp}] = [Z][J_{ip}] + [Z][ZJ_{pn}][J_o] + [Z][ZK_{pn}][K_o] \quad (26)$$

where

$$Z_{np} = \frac{-k_0 \eta_0}{4} H_0^{(1)}(k_0 |\bar{r}_n - \bar{r}_p|) d\bar{r}_p \quad (\bar{r}_n \in c, \bar{r}_p \in S), \quad (27)$$

Substitute the Equation (26) into (21), the integral Equations (21) and (22) can be converted into a set of equations of the induced electric current  $J_o$  and magnetic current  $K_o$  on the target surface. So instead of solving the coupling EFIEs of target and rough surface in the convention MoM, in this hybrid method it is only need to calculate the EFIEs of target only, which will greatly reduce the computational time and memory requirements.

## 2.2. Truncation of the Underlying Rough Surface

When taking account of the scattering contribution from the rough surface towards the target, it is unnecessary to consider the contribution of the whole length of the rough surface, but only the rough surface near the target, for lots of rough surface scattering cannot incident on the target. According to the KA [21, 24], the bistatic scattering from the moderate underlying rough surface is dominated in the specular direction of the mean plane, so a small section of rough surface toward the target in that direction, which is taken as  $L1$ :  $\{x \in (-g/2, \sin \theta_i (h / \cos \theta_i - 1.5r \tan \theta_i - 1.5r / \tan \theta_i))\}$  as shown in Figure 2, is only needed to take account of the secondary scattering contribution driven by the tapered wave from the underlying rough surface to the target. Taking the scattering from the target as an incident wave to the underlying rough surface, because the moderate underlying rough surface is random and is created by Monte Carlo

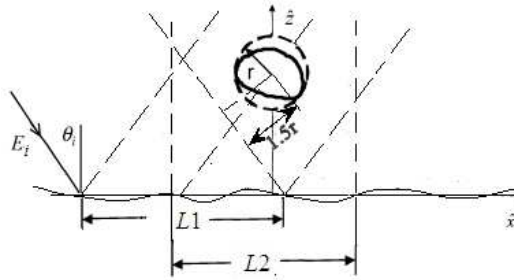


**Figure 2.** Truncation of the underlying rough surface to calculate the surface scattering account to the target.

realization, there is only small section of rough surface whose local specular reflection has some chance to incident on the target. The section is taken as  $L2: \{x \in (-2r, 2r)\}$  as shown in Figure 2 to take account of the secondary scattering contribution driven by the scattering field of the target from the underlying rough surface to the target. It is worth noting that the above limits of  $L1$  and  $L2$  are only feasible for surface with roughness not big. So the underlying rough surface scattering account to the target can be written as

$$ik_0\eta_0A_s(\bar{r}) = [Z][J_{sp}] = A_{s1} + A_{s2} \tag{28}$$

where  $A_{s1}$  is the secondary scattering contribution driven by the tapered wave, and  $A_{s2}$  is the secondary scattering contribution due to the target presence, they can be expressed as

$$A_{s1} = [Z_{np}][J_{ip}] \quad (\bar{r}_n \in c, \bar{r}_p \in L1) \tag{29}$$

$$A_{s2} = [Z_{np}][ZJ_{pn}][J_o] + [Z_{np}][ZK_{pn}][K_o] \quad (\bar{r}_n \in c, \bar{r}_p \in L2) \tag{30}$$

Substitute the Equation (28) into (21), the integral equations can be converted into a set of equations of the induced electric current  $J_o$  and magnetic current  $K_o$  on the target surface

$$\begin{aligned} &([Z_j] + [Z][ZJ_{pn}])[J_o] + ([Z_k] + [Z][ZK_{pn}])[K_o] \quad (\bar{r}_p \in L2) \\ &= -E_i(\bar{r}) - [Z][J_{ip}] \quad (\bar{r}_p \in L1) \end{aligned} \tag{31}$$

$$[Z_j^{(d)}][J_o] + [Z_k^{(d)}][K_o] = 0 \tag{32}$$

where  $Z_j$  and  $Z_j^{(d)}$  are the external and internal original impedance matrices of the induced electric current, respectively, and  $Z_k$  and  $Z_k^{(d)}$  are the external and internal original impedance matrices of the induced magnetic current, respectively. They are the exact impedance matrices of the target when there is only target in the free space

and can be directly determined by Equations (21) and (22). From a physics point of view Equation (31) is a modified EFIE of the target due to the presence of the underlying rough surface.  $[Z][ZJ_{pn}]$  and  $[Z][ZK_{pn}]$  are the additional impedance matrices of the induced electric current and induced magnetic current respectively because of the multiple interactions between the target and the underlying rough surface. While  $-[Z][J_{ip}]$  is the additional voltage matrix caused by the secondary scattering field of the rough surface driven by the tapered incident wave.

The induced electric current  $J_o$  and magnetic current  $K_o$  can be directly calculated by Equations (31) and (32). Once these induced currents on the target surface have been determined, the induced current  $J_s$  on the rough surface can be obtained from Equation (17). Then the scattering field can be calculated by

$$E_s(\bar{r}) = ik_0\eta_0 A_s(\bar{r}) + ik_0\eta_0 A_o(\bar{r}) - \left( \frac{\partial F_x(\bar{r})}{\partial z} - \frac{\partial F_z(\bar{r})}{\partial x} \right), \quad (33)$$

and the Bi-NRCS is defined as [13]

$$\sigma(\theta_s, \theta_i) = \lim_{\rho \rightarrow \infty} \rho \frac{|E_s(\theta_s, \theta_i)|^2}{g\sqrt{\pi/2} \cos \theta_i \left[ 1 - \frac{1+2 \tan^2 \theta_i}{2k^2 g^2 \cos^2 \theta_i} \right]}, \quad (34)$$

where  $\rho$  is the distance between the coordinate origin and the field point in far-field region.

### 3. NUMERICAL RESULTS

In order to verify the accuracy and efficiency of the proposed method, we consider a dielectric cylindrical target with relative complex permittivity  $\varepsilon_d = 2$  and radius  $r$  at the altitude  $h$  above a PEC Gaussian rough surface with RMS height  $\delta = 0.1\lambda$  and correlation length  $l = 4\lambda$ . The rough surface is created by 100 Monte Carlo realizations in the following numerical simulations. When the radius  $r = \lambda$  and altitude  $h = 4\lambda$ , the incident angles are  $\theta_i = 20^\circ$  and  $\theta_i = 60^\circ$  respectively. The surface lengths  $L$  are determined by Equations (3)–(5) and (7) without considering of the largest scattering angle. In the conventional MoM based on the coupling EFIEs of the induced currents both on the target and the rough surface, the number of unknowns are  $2N + P$ . Using the hybrid method, however, only the EFIEs of the induced currents on the target with  $2N$  unknowns are required. Since the unknown number on the surface is much greater than on the target, the computational time and memory requirements are greatly reduced as shown in Table 1. Figures 3 and 4 show the Bi-NRCSs computed by

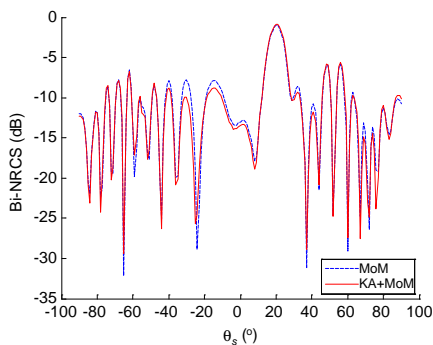


**Figure 3.** Bistatic NRCS comparison of a cylinder with  $r = \lambda$  and  $h = 4\lambda$  above the Gaussian rough surface ( $\theta_i = 20^\circ$ ).

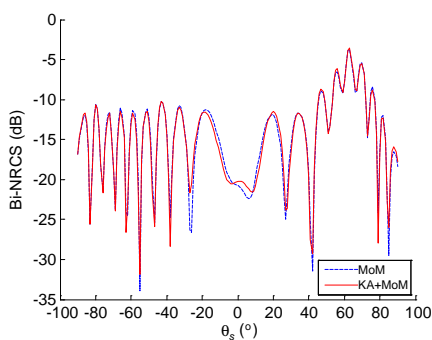


**Figure 4.** Bistatic NRCS comparison of a cylinder with  $r = \lambda$  and  $h = 4\lambda$  above the Gaussian rough surface ( $\theta_i = 60^\circ$ ).

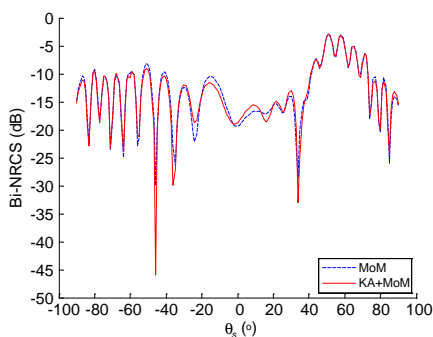


**Figure 5.** Bistatic NRCS comparison of a cylinder with  $r = 1.5\lambda$  and  $h = 4\lambda$  above the Gaussian rough surface ( $\theta_i = 60^\circ$ ).

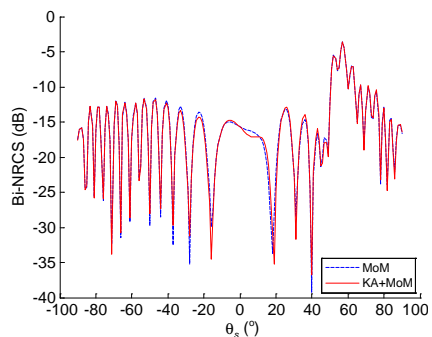


**Figure 6.** Bistatic NRCS comparison of a cylinder with  $r = \lambda$  and  $h = 6\lambda$  above the Gaussian rough surface ( $\theta_i = 60^\circ$ ).

the conventional MoM and the hybrid method with different incident angles. It can be seen that the results of the two methods are well matched. Also we can clearly see from Table 1 that the rough surface length required for this composite model becomes larger with larger incident angle, and the ratio of the computational time and memory requirements by the hybrid and MoM is becoming smaller as incident angle increases.

In order to further verify the hybrid method, we consider another two cases. One is for the bigger radius ( $r = 1.5\lambda$ ), where the coupling

**Table 1.** Comparison of the effectiveness of MoM and the hybrid method.

$r$	$h$	$\theta_i$	$L$	method	Unknown number	Computational time	Memory requirements
$\lambda$	$4\lambda$	$20^\circ$	$60\lambda$	MoM	788	47.890 s	16.2 MB
				KA + MoM	188	29.560 s	2.52 MB
$\lambda$	$4\lambda$	$60^\circ$	$142.85\lambda$	MoM	1616	214.8412 s	73.0 MB
				KA + MoM	188	68.9245 s	4.99 MB
$1.5\lambda$	$4\lambda$	$60^\circ$	$158.85\lambda$	MoM	1870	273.8609 s	95.9 MB
				KA + MoM	282	111.2408 s	8.75 MB
$\lambda$	$6\lambda$	$60^\circ$	$198.28\lambda$	MoM	2170	373.7431 s	133 MB
				KA + MoM	188	90.2959 s	6.63 MB

among the target and the rough surface becomes stronger. In this case, the Bi-NRCSs computed by the two methods are illustrated in Figure 5 and the computational time and memory requirements are presented in Table 1. Obviously, compared to the case of smaller radius, the computational time and memory requirements of the hybrid method are greatly increasing due to the large increasing of the unknowns of the induced currents on the target as shown in Table 1. It is worth noting that once the target becomes bigger, more surface length is also required, but the ratio of the unknown increased on the target is much bigger than on the rough surface. So compared with the case of smaller radius, the ratio of the computational time and memory requirements by the hybrid and MoM becomes bigger. The other case is for the target at higher altitude ( $h = 6\lambda$ ), where the coupling among the target and rough surface becomes weaker. In this case, the surface length becomes larger, so the unknowns of induced current on the rough surface are increasing. As a result, the ratio of the computational time and memory requirements by the hybrid method and MoM are reduced as shown in Table 1. The Bi-NRCS computed by the two methods are illustrated in Figure 6.

#### 4. CONCLUSION

A hybrid method of analytic KA and numerical MoMs is developed to solve the composite scattering model of a dielectric target above a PEC rough surface. Using the KA method, the surface field on the rough surface is analytically expressed by the tapered wave and induced current  $J_o$  and  $K_o$  on the target. Then the electric field integral equations of the induced currents on the target can be derived, so

that unknowns would be required only on the dielectric target, which will greatly reduce the computational time and memory requirements. Furthermore, a small portion of the rough surface towards the target along the specular direction for the secondary scattering driven by the tapered incident wave and a small surface portion directly under the target for the secondary scattering driven by the scattering field of the target are taken to speed up computation of the scattering contribution from the rough surface to the target. A cylindrical target is located above the rough surface as an example. Compared with the results of the MoM, numerical examples demonstrate the effectiveness and accuracy of this hybrid KA-MoM method.

It is worth noting that this hybrid method cannot deal with composite model with grazing incidence, which is due to the limitations of the KA algorithm [25]. And this hybrid method can be extended to solve the 3-D composite scattering problem of a target above a random rough surface.

## ACKNOWLEDGMENT

The research is supported in part by 41176156 and 51207060 NSFC, P. R. China, and by 863 Program (the National High Technology Research and Development Program of China) No. 2010AA122200.

## REFERENCES

1. Johnson, J. T., "A study of the four-path model for scattering from an object above a half space," *Micro. Opt. Techn. Let.*, Vol. 30, 130–134, 2011.
2. Guo, L. X. and Z. Wu, "Application of the extended boundary condition method to electromagnetic scattering from rough dielectric fractal sea surface," *Journal of Electromagnetic Waves and Applications*, Vol. 18, No. 9, 1219–1234, 2004.
3. Wang, X., C. F. Wang, and Y. B. Gan, "Electromagnetic scattering from a circular target above or below rough surface," *Progress In Electromagnetics Research*, Vol. 40, 207–227, 2003.
4. Li, Z. and Y. Q. Jin, "Bistatic scattering from a fractal dynamic rough sea surface with a ship presence at low grazing-angle incidence using the GFBM/SAA," *Micro. Opt. Techn. Let.*, Vol. 31, 146–151, 2001.
5. Li, Z. and Y. Q. Jin, "Bistatic scattering and transmitting through a fractal rough surface with high permittivity using the physics based two-grid method in conjunction with the forward-backward

- method and spectrum acceleration algorithm,” *IEEE Trans. Antenn. Propag.*, Vol. 50, 1323–1327, 2002.
6. Liu, P. and Y. Q. Jin, “The finite-element method with domain decomposition for electromagnetic bistatic scattering from the comprehensive model of a ship on and a target above a large scale rough sea surface,” *IEEE Trans. Geosci. Remote*, Vol. 42, 950–956, 2004.
  7. Liu, Z., R. J. Adams, and L. Carin, “Well-conditioned MLFMA formulation for closed PEC targets in the vicinity of a half space,” *IEEE Trans. Antenn. Propag.*, Vol. 51, 2822–2829, 2003.
  8. Li, L., J. Q. He, Z. J. Liu, and L. Carin, “MLFMA analysis of scattering from multiple targets in the presence of a half-space,” *IEEE Trans. Antenn. Propag.*, Vol. 51, 810–819, 2003.
  9. Kubicke, G., C. Bourlier, and J. Saillard, “Scattering by an object above a randomly rough surface from a fast numerical method: Extended PILE method combined with FB-SA,” *Waves in Random and Complex Media*, Vol. 18, 495–519, 2008.
  10. Guo, L. X., Y. Liang, and Z. S. Wu, “A study of electromagnetic scattering from conducting targets above and below the dielectric rough surface,” *Opt. Express*, Vol. 19, 5785–5801, 2011.
  11. Ye, H. X. and Y. Q. Jin, “Fast iterative approach to difference scattering from the target above a rough surface,” *IEEE Trans. Geosci. Remote*, Vol. 44, 108–115, 2006.
  12. Ye, H. X. and Y. Q. Jin, “Fast iterative approach to the difference scattering from a dielectric target above a rough surface,” *Sci. China. Ser. G*, Vol. 48, 723–738, 2005.
  13. Chen, H. and W. J. Ji, “Fast calculation of EM scattering from a dielectric target above the dielectric Gauss rough surface based on the cross coupling iterative approach,” *2011 Cross Strait Quad-Regional Radio Science and Wireless Technology Conference*, 168–170, 2011.
  14. Li, J., L. X. Guo, and H. Zeng, “FDTD investigation on bistatic scattering from a target above two-layered rough surfaces using UPML absorbing condition,” *Progress In Electromagnetics Research*, Vol. 88, 197–211, 2008.
  15. Zhang, Y., Y. E. Yang, H. Braunisch, and J. A. Kong, “Electromagnetic wave interaction of conducting object with rough surface by hybrid SPM/MoM technique,” *Progress In Electromagnetics Research*, Vol. 22, 315–335, 1999.
  16. He, S. Y. and G. Q. Zhu, “A hybrid MM-PO method combing UV technique for scattering from two-dimensional target above a

- rough surface,” *Micro. Opt. Techn. Let.*, Vol. 49, No. 12, 2957–2960, 2007.
17. Ye, H. X. and Y. Q. Jin, “A hybrid analytic-numerical algorithm of scattering from an object above a rough surface,” *IEEE Trans. Geosci. Remote*, Vol. 45, 1174–1180, 2007.
  18. Wang, R., L. X. Guo, J. Ma, and Z. S. Wu, “Hybrid method for investigation of electromagnetic scattering from conducting target above the randomly rough surface,” *Chinese. Phys. B*, Vol. 18, 1503–1602, 2009.
  19. Yang, W., Z. Q. Zhao, C. H. Qi, W. Liu, and Z. P. Nie, “Iterative hybrid method for electromagnetic scattering from a 3-D object above a 2-D random dielectric rough surface,” *Progress In Electromagnetics Research*, Vol. 117, 435–448, 2011.
  20. Wu, Z. S., J. J. Zhang, and L. Zhao, “Composite electromagnetic scattering from the plate target above a one-dimensional sea surface: Taking the diffraction into account,” *Progress In Electromagnetics Research*, Vol. 92, 317–331, 2009.
  21. Ticconi, F., L. Pulvirenti, and N. Pierdicca, “Models for scattering from rough surfaces,” *Electromagnetic Waves*, V. Zhurbenko (ed.), Chapter 10, 203–226, InTech, 2011.
  22. Ye, H. and Y. Q. Jin, “Parameterization of the tapered incident wave for numerical simulation of electromagnetic scattering from rough surface,” *IEEE. Trans. Antenn. Propag.*, Vol. 50, 1361–1367, 2005.
  23. Peterson, A. F., S. L. Ray, and R. Mittra, *Computational Methods for Electromagnetics*, 37–94, IEEE Press, New York, 1997.
  24. Thorsos, E. I., “The validity of the Kirchhoff approximation for rough surface scattering using a Gaussian roughness spectrum,” *J. Acoust. Soc. Am.*, Vol. 83, 78–92, 1988.
  25. Brown, G. S., “The validity of shadowing corrections in rough surface scattering,” *Radio Science*, Vol. 19, No. 6, 1461–1468, 1984.